

# Study on the Compaction Characteristics of Loessial Silt Using Electrochemical Impedance Spectroscopy

Jie Li<sup>1</sup>, Ruizhen Xie<sup>2</sup>, Pengju Han<sup>1,3,\*</sup>, Xiaohong Bai<sup>1,3,\*</sup>

<sup>1</sup>College of civil engineering, Taiyuan University of Technology, Taiyuan 030024, China

<sup>2</sup>Mechanics Institute, Jinzhong University, Jinzhong 030619, China

<sup>3</sup>Shanxi Key Laboratory of Geotechnical and Underground Engineering, Taiyuan 030024, China

\*E-mail: [bxhong@tyut.edu.cn](mailto:bxhong@tyut.edu.cn); [13834569544@163.com](mailto:13834569544@163.com)

Received: 2 March 2020 / Accepted: 23 March 2020 / Published: 10 June 2020

The measurement technique of electrochemical impedance spectroscopy (EIS) was applied to study the compaction characteristics of loessial silt. A series of compaction curves (single-peak curves) were obtained under different compaction energies. It was found that when the compaction energy ( $E$ ) is 2013.7 kJ/m<sup>3</sup>, the optimal water content ( $w_{opt}$ ) is 14.3%, and the maximum dry density ( $\rho_{dmax}$ ) is 1.90 g/cm<sup>3</sup>; when  $E$  is 2684.9 kJ/m<sup>3</sup>,  $w_{opt}$  and  $\rho_{dmax}$  is 13.6% and 1.95 g/cm<sup>3</sup>, respectively. From an electrochemical test of compacted soil samples with  $E = 2013.7$  kJ/m<sup>3</sup> and five different water contents, the following results were obtained: the electrochemical characteristics of compacted soil are closely related to the water content. The electrochemical impedance spectroscopy can be effectively measured only when the water content of the soil samples exceeds than the optimal water content ( $> w_{opt} - 2\%$ ). The solution resistance is directly related to the water content, but not to the density of the soil sample. The capacitance and resistance of the inner porous layer close to the electrode are the largest at the optimal water content, which is related to the density and continuity of the solid particles. The charge transfer resistance decreases with the increasing water content and eventually becomes stable. Therefore, the compactness of loess-filled soil can be quickly and effectively reflected using the EIS.

**Keywords:** EIS, loessial silt, compaction curve, water content

## 1. INTRODUCTION

With the continuous development of infrastructure in central and western China, construction land is increasingly scarce. To solve this problem, filling engineering is used to expand the construction land in many places. Due to regional and economic limitations, local materials are often used for filling. The loess widely distributed in central and western of China is often used as the preferred filler for roadbeds, foundations and other construction sites [1]. Loess is a typical special soil with complex engineering properties, and engineering diseases emerge in an endless succession, which is especially

for loessial silt [2, 3]. Due to the insufficient compaction of loess-like silt, subgrade subsidence occurred in many places of the yellow flood plain section of the Beijing-Kowloon railway [4]. In filling engineering, the soil needs to be reshaped and compacted to change its original structure and physical and mechanical characteristics [5, 6]. To ensure the strength and stability of the backfill, the factor of compaction is often used as the index of controlling quality, which is defined as the ratio of dry density  $\rho_d$  after compaction of field packing to the maximum dry density  $\rho_{dmax}$  of a laboratory compaction test [7]. Compaction and vibration are usually used to reinforce the soil in the field. In the laboratory, a compaction curve is obtained by the compaction test.

The deviation of field test is large, and the compaction quality of soil cannot be characterized from the microscopic mechanism and pore structure. Electrochemical impedance spectroscopy (EIS), as a non-destructive testing method, is widely used in study of electrode process, electrical double layer, solid electrolytes and other mechanisms [8, 9]. Soil is a heterogeneous medium, including solid particles, air and water, which can form an electrochemical system. An increasing number of scholars have extended electrochemical testing technology to geotechnical engineering. However, research on the basic law of the electrochemical characteristics of loessial silt remains in the preliminary stage [10-13]. Yan [14] studied the changes in physical mechanics and electrochemical properties of silty soils with different pH values. Han et al. [15] studied the mechanical properties of acidic and alkaline silt using electrochemical impedance spectroscopy. The interaction of clay and pore water in loessial silt results in the formation of an electrical double layer. The changes in the thickness of the electrical double layer will affect the intergranular stress the electrochemical behavior of the soil [16]. EIS is an electrochemical technique that studies a system under the action of an alternating current by the equivalent circuit, which can comprehensively reflect the conductive path and interface characteristics of the system, especially the structure of electrical double layer [17, 18]. Therefore, it is feasible to quickly reflect the compaction quality and compaction mechanism of silt by means of EIS testing.

To further study the electrochemical behavior of compacted loessial silt, typical loess soil in Shanxi province was selected for a laboratory compaction test. The electrochemical test of compacted soil samples with different water contents was performed to reveal the compaction mechanism of soil from an electrochemical perspective.

## 2. EXPERIMENTAL PROCEDURE

### 2.1 Experimental materials and pretreatment

The soil in the test was taken from a filling area in Shanxi province of China, where loess is widely distributed. The basic physical properties of soil samples were determined in accordance with the “Standard for Soil Test Methods” (GB/T50123-2019) [19], and the results are listed in table 1. The plasticity index ( $I_p$ ) of the soil is less than or equal to 10, and its particle content with particle size greater than 0.075 mm is  $14.7\% < 50\%$ , so it is named silt according to the “Code for Design of Building Foundation” [20]. The specific gravity of the soil particles ( $d_s$ ) is 2.70. The liquid limit ( $W_L$ ) and the plastic limit ( $W_P$ ) is 25.5% and 16.6%, respectively.

**Table 1.** The basic physical properties of testing soil

Grain size (mm)/%				$d_s$	$W_L/\%$	$W_P/\%$	$I_P$
0.25~0.075	0.075~0.05	0.05~0.005	<0.005				
1.8	37.4	52.6	8.2	2.70	25.5	16.6	8.9

## 2.2. Experimental method

### 2.2.1 Compaction test

A heavy compaction test with a JDS-3 portable compactor is used in this paper. The compaction energy ( $E$ ) is  $E_1 = 2013.7 \text{ kJ/m}^3$  and  $E_2 = 2684.9 \text{ kJ/m}^3$ . The water used for the test is ordinary tap water. Five groups of compaction samples with different water contents ( $w$ ) under the given compaction energy was tested. The water content values were prepared according to the plastic limit ( $W_P$ ) of soil samples under each compaction energy. The dry soil was thoroughly mixed with water and allowed to sit for 24 hours. According to the steps specified in the “Standard for Soil Test Methods” (GB/T50123-2019) [19]. The compaction curves of soil under different compaction energies were measured.

In the test, the compaction energy ( $E$ ) and the number of soil layers ( $n$ ) were given. According to the volume ( $V$ ) of the solid cylinder, the hammer gravity ( $G$ ), and the drop distance ( $d$ ) of the hammer, the number of hits ( $N$ ) required for each layer of soil can be calculated based on Formula (1), and rounded the calculation results. The required compaction parameters listed in Table 2.

$$N = EV / Gdn \quad (1)$$

**Table 2** The compaction parameter under different compaction energy

$E \text{ (kJ/m}^3\text{)}$	$G \text{ (kN} \times 10^{-3}\text{)}$	$d \text{ (m)}$	$V \text{ (m}^3\text{)}$	$n$	$N$
2013.7	86.06	0.45	$0.5385 \times 10^{-3}$	4	7
2684.9	114.75	0.45	$0.5385 \times 10^{-3}$	4	7

### 2.2.2 Electrochemical impedance spectroscopy

A CS350 electrochemical workstation was used for the test, with a sinusoidal AC excitation signal amplitude of 5 mV and a scanning frequency range of  $10^{-2}$ - $10^5$  Hz. The electrochemical behavior of five groups of compaction samples with different water contents under the given compaction energy was tested. The size of the sample to be tested is 61.8 mm in diameter and 20 mm in height. The EIS tests are performed under the two-electrode system, with working electrode (WE, the copper sheet of 100 mm×100 mm×1 mm), counter electrode (CE, the copper sheet of 100 mm×100 mm×1 mm). And the glass sheet affixed with copper sheet, with size of 100 mm×100 mm×2 mm, as shown in figure 1. The Nyquist diagram, the Bode diagram and compaction parameters of the soil were analyzed.

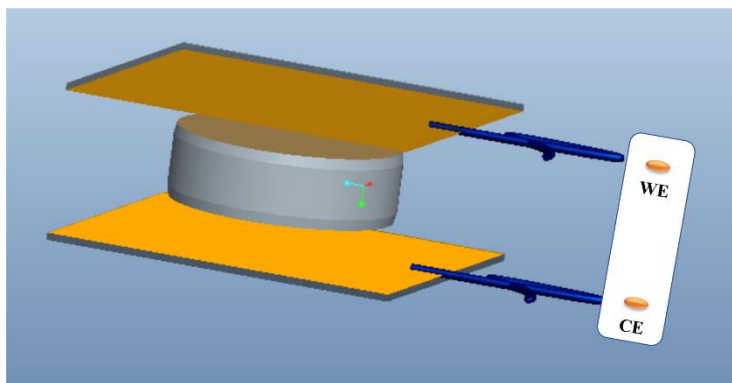


**Figure 1.** Experimental setup diagram

### 3. RESULTS AND DISCUSSION

#### 3.1 Compaction curves of loessial silt

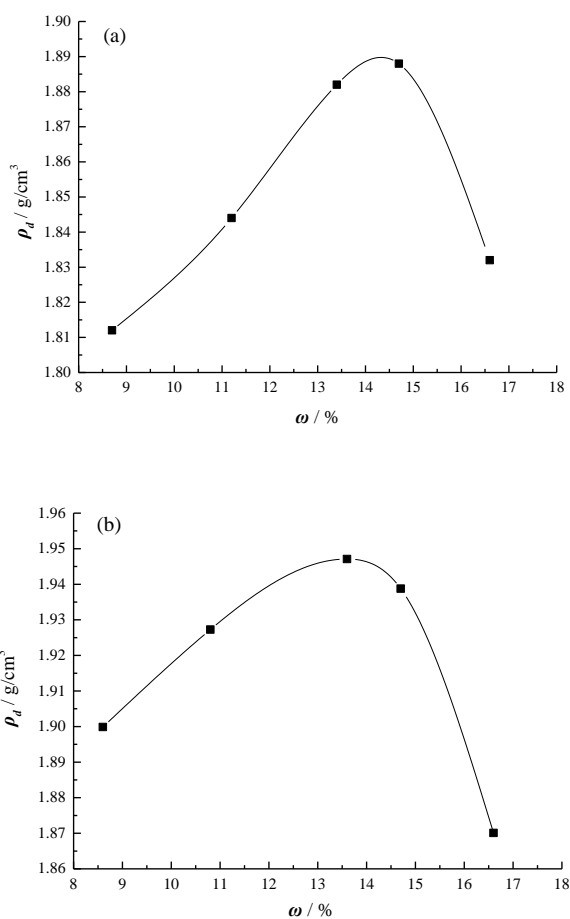


**Figure 2.** Compaction curves of different compaction energies: (a)  $E_1 = 2013.7 \text{ kJ/m}^3$ , (b)  $E_2 = 2684.9 \text{ kJ/m}^3$

According to different compaction energies and the corresponding compaction steps, compaction curves under two types of compaction energies ( $E_1$ ,  $E_2$ ) were obtained. The corresponding optimal water content ( $w_{opt}$ ) and maximum dry density ( $\rho_{dmax}$ ) were determined. The compaction curves are shown in Figure 2.

Figure 2 shows that the compaction curve presents a single-peak curve regardless of the compaction energy. The dry density ( $\rho_d$ ) of the soil samples first increases and subsequently decreases with increasing water content ( $w$ ). The peak value is the maximum laboratory dry density ( $\rho_{dmax}$ ) under the corresponding compaction energy, and the corresponding water content is the optimal water content ( $w_{opt}$ ) under the given compaction energy. And it agrees with the general characteristics of fine-grained soil compaction [21]. When the water content is low, there is a large friction resistance between particles, and the soil is not easy to be compacted. As the water content increases, water on the particles surface begins to play a lubricating role, reducing the resistance between grains, the soil becomes compacted easily. And the dry density of the soil increases. When water contents exceeding the optimum level ( $> w_{opt}$ ), the air in soil is sealed and cannot dissipate during compacting. When the impact force is applied to the soil, most of the force is borne by pore water and pore gas, so the dry density of the soil decreases.

According to Figure 1, when  $E_1 = 2013.7 \text{ kJ/m}^3$ ,  $w_{opt} = 14.3\%$ , and  $\rho_{dmax} = 1.90 \text{ g/cm}^3$ ; when  $E_2 = 2684.9 \text{ kJ/m}^3$ ,  $w_{opt} = 13.6\%$ , and  $\rho_{dmax} = 1.95 \text{ g/cm}^3$ . This may be related to the water distribution in loess and the electrical double layer around the grains [22, 23]. The electrical double layer will change the action of interparticle forces.

### 3.2 EIS analysis of the compacted loessial silt with different water contents

#### 3.2.1 Nyquist diagram and Bode diagram

Based on the above compaction test results in this paper, regardless of the compaction energy, the variation law of the dry density with the water content in the compaction curve is a single-peak curve. Therefore, a soil sample with different water contents on the compaction curve can be selected for electrochemical analysis. The electrochemical behavior of soil samples with different water content, under certain compaction energy, was determined and analyzed. The compaction energy  $E_1 = 2013.7 \text{ kJ/m}^3$  was selected for analysis. Five samples of compacted loessial silt with different water contents,  $S_1$  ( $w = 8.7\%$ ),  $S_2$  ( $w = 11.2\%$ ),  $S_3$  ( $w = 13.4\%$ ),  $S_4$  ( $w = 14.7\%$ ) and  $S_5$  ( $w = 16.6\%$ ), were tested by electrochemical impedance spectroscopy. The Nyquist diagram and Bode diagram are shown in Figure 2 and Figure 3, respectively. The surface of sample  $S_1$  could not effectively contact the test electrode due to too little water content, which resulted in the Nyquist diagram of soil could not present capacitive loop. Therefore, only Bode diagram was compared and analyzed in this paper.

The Nyquist diagram (Figure 3) show that the EIS of each compacted loessial silt at different water contents consists of a capacitive loop and a  $45^\circ$  oblique line. The capacitive loop is not obvious in the high-frequency region, which may be related to the electrical double layer structure around the clay in the soil [24, 25]. Compacted loessial silt is an unsaturated soil with three phases: solid, liquid and air, which provides sufficient oxygen environment for the cathode reaction of electrochemical process and increases the tendency of local corrosion [26]. When the water content is low, there is less free water in

the pores, the conductive paths in the soil are mainly a few continuous liquid phase paths, and the overall impedance of soil is higher. When the water content increases, the free water among soil particles increases. In addition to the continuous liquid phase paths, the electrical double layer around the clay also forms part of the conductive path. Therefore, the overall impedance of the soil decreases. When the water content reaches saturation, the compacted loessial silt as a whole is in the solid and liquid state. The Bode diagram also show that the modulus of compacted loessial silt significantly decreases with increasing water content (Figure 4).

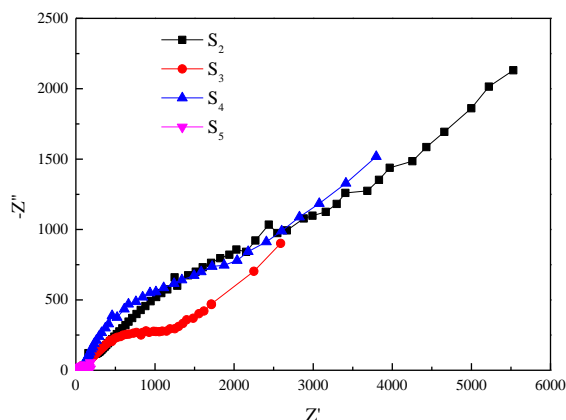


**Figure 3.** Nyquist diagram of compacted loessial silt with different water contents:  $S_2$  ( $w = 11.2\%$ ),  $S_3$  ( $w = 13.4\%$ ),  $S_4$  ( $w = 14.7\%$ ) and  $S_5$  ( $w = 16.6\%$ )

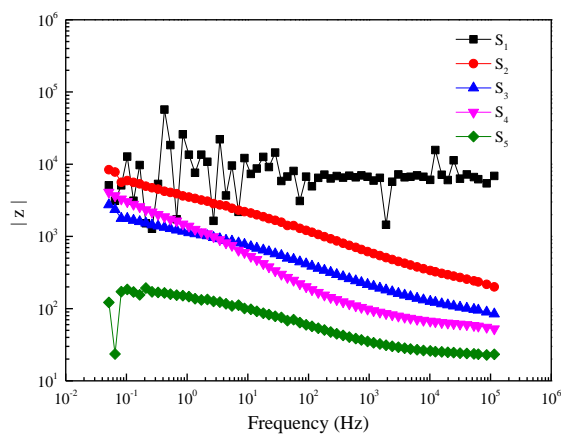


**Figure 4.** Bode diagram of compacted loessial silt with different water contents:  $S_1$  ( $w = 8.7\%$ ),  $S_2$  ( $w = 11.2\%$ ),  $S_3$  ( $w = 13.4\%$ ),  $S_4$  ( $w = 14.7\%$ ) and  $S_5$  ( $w = 16.6\%$ )

### 3.2.2 Electrochemical impedance analysis of compacted loessial silt

The equivalent circuit  $R(C(R(Q(RW))))$  can be used as the basic equivalent circuit of compacted loessial silt (Figure 5). The  $R_e$  is the solution resistance,  $(R_{ct}W)Q_{dl}$  is the capacitance of electrical double layer and Faradaic resistance formed at the interface of the electrode and pore water,  $(CsRs)$  is the capacitance and resistance of the inner porous layer close to the electrode, and the capacitance formed by soil adsorption is represented by  $C_s$  in compacted loessial silt [27].

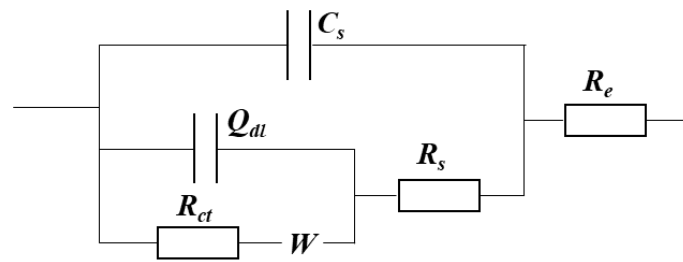


**Figure 5.** Compacted loessial silt equivalent circuit model

The EIS results of compacted loessial silt with different water contents were fitted. The fitting software is ZSimDemo3.30, and the fitting results are shown in Table 3.

**Table 3.** EIS fitting results with different water contents

No.	$R_e$ ( $\Omega \cdot \text{cm}^2$ )	$R_{ct}$ ( $\Omega \cdot \text{cm}^2$ )	$Q_{dl}$		$C_s$ ( $\text{F} \cdot \text{cm}^{-2}$ )	$R_s$ ( $\Omega \cdot \text{cm}^2$ )	$W$ ( $\text{S} \cdot \text{s}^{0.5} \cdot \text{cm}^{-2}$ )
			$Y_0(\text{S} \cdot \text{s}^{-n} \cdot \text{cm}^{-2})$	$n$			
S <sub>2</sub>	159.25	86.05	1.7E-4	0.21	3.4E-9	186.3	1.2E-5
S <sub>3</sub>	77.86	61.2	1.6E-4	0.42	6.7E-9	1526	1.5E-3
S <sub>4</sub>	50.311	25.96	1.8E-4	0.55	4.2E-8	3739	9.6E-4
S <sub>5</sub>	22.95	20.79	1.4E-3	0.43	6.2E-9	192.8	8.4E-4

The results show that the  $R_e$  decreases with increasing water content. The charge transfer resistance  $R_{ct}$  decreases with increasing water content. When the water content is close to the optimal water content. The values of  $n$  are all below 0.6, indicating that the electrical double layer at the electrode interface deviate from the ideal capacitance to some extent. With a decrease in the water content (when  $w < w_{opt}$ ), the deviation degree of interfacial capacitance from the ideal capacitance significantly increases. When  $w > w_{opt}$ , with an increase in the water content, the same law remains, which is related to the pore fluid state at the electrode interface. The change of  $C_s$  with the increasing water content increases first and then decreases, and the order of magnitude is basically E-9 ~ E-8, the numerical order of the diffusion element  $W$  is E-5 ~ E-3. The  $R_s$  first increases and subsequently decreases with increasing water content, which may be due to different compact levels of soil particles under different water content conditions. The continuity of particles causes the changes in  $R_s$ .

The two-electrode system consists of one loop, consisting of the working electrode (WE) and counter electrode (CE) for transporting electrons. In soil, the current flows through an overall cross-sectional area that is linked to the saturation level [28]. The conductive path in soil mainly includes the following [29]: 1. a solid-liquid alternating interface formed by discontinuous solid-phase sand particles and pore fluid; 2. a solid-liquid alternating interface formed by continuous solid-phase sand particles and liquid bridge; and 3. a continuous liquid phase between sand particles. All three conductive paths are closely related to the pore water in the soil.

3.3 Correlation analysis between the EIS fitting results and compaction curves

There is a certain correlation between the EIS characteristics of the soil and the compaction curves, both of which are closely related to the water content.

The  $R_s$  also first increases and subsequently decreases with the increase in water content, as shown in Figure 6. When the water content is 14.7% (approximately the  $w_{opt}$ ),  $R_s$  reaches the maximum value. A higher dry density  $\rho_d$  corresponds to a more compacted loessial silt. The variation law of  $R_s$  with the water content is similar to that of  $\rho_d$  with the water content. The results show that the  $R_s$  is closely related to the density of the soil.

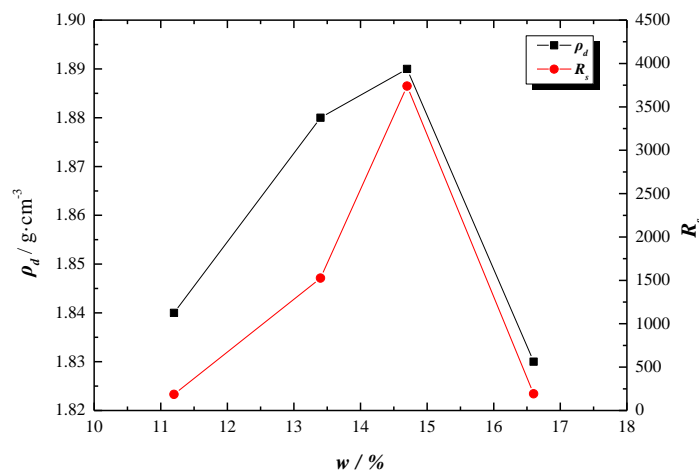


Figure 6.  $\rho_d$ ,  $R_s$  relation curve with the water content

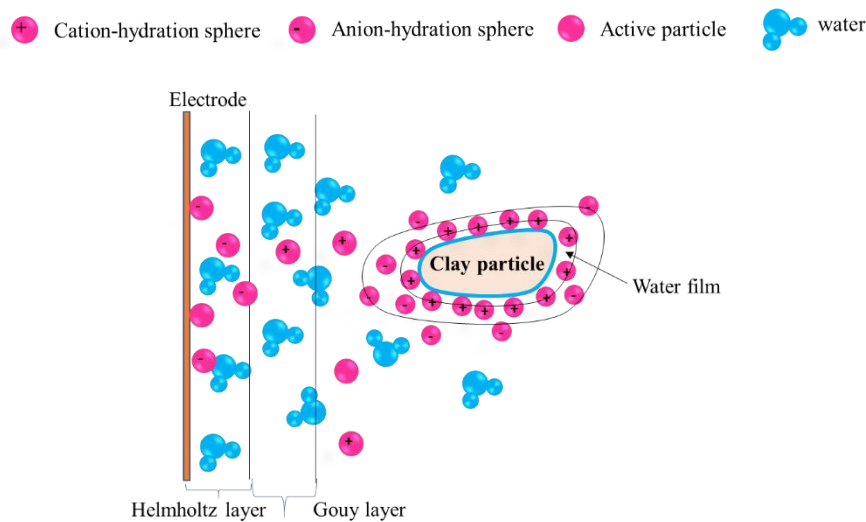


Figure 7. Interface structure of the compacted loessial silt electrode

When the soil density increases, the more continuous solid particles correspond to greater resistance of the solid particles as a whole. When the soil dry density reaches the peak value, with increasing water content, free water among the soil particles increases. Too much free water breaks the continuity between particles. Moreover, when the compaction impact force is generated, this water will form excessive pore water pressure, and the particles are not easily compacted. The overall resistance

formed by continuous solids decreases. And the  $C_s$  is closely related to the density of the soil too, with the increase of water content, it increases first and then decreases.

Figure 7 shows the interface structure of the compacted loessial silt electrode, which mainly includes the electrical double layer at the electrode-solution interface and the water film at the particle-solution interface [30, 31]. At the interface of metal electrode and pore water, electrical double layer can be divided into Helmholtz layer and Gouy layer [31].

Table 3 show that the  $R_{ct}$  continuously decreases with increasing water content. However, when  $w \geq w_{opt}$ , the reduction range significantly decreases. The charge transfer is closely related to the pore water content. In addition, silt is a fine-grained soil, whose cohesion and adhesion affect the difficulty of the charge transfer [32, 33]. Under the same compaction energy, when the water content is low ( $w < w_{opt}$ ), the electrical double layer on the surface of the soil particles (Figure 7) is thin and has a strong ability to absorb charge. The whole charge of compacted loessial silt is not easy to transfer,  $R_{ct}$  is larger, and the soil is not easy to compaction. As the water content increases, water begins to play a lubricating role in the pores. The electrical double layer on the surface of soil particles is thickened, and the intergranular resistance is reduced. Therefore, the soil is easy to compact, but it will still affect the charge transfer, and the impact degree is reduced. When the water content continues to increase ( $w > w_{opt}$ ), the intergranular pores may be expanded by water, the intergranular resistance continues to decrease, and the surface of the soil particles is less able to absorb charge, so the charge can be freely transferred in the pore water. Therefore, as the water content continues to increase, the difficulty of charge transfer decreases, so the  $R_{ct}$  decreases. When the water content is much higher than the optimal water content,  $R_{ct}$  tends to be stable because when the water content continues to increase beyond the optimal water content, the soil tends to saturation. The surface of soil particles forms a stable electrical double layer, and the degree of difficulty of charge transfer in pore water becomes stable. Therefore, the reduction in  $R_{ct}$  is not significant.

When water content increases, the conductivity of pore water solution is enhanced, and the corresponding solution resistance  $R_e$  is smaller, as shown in Table 3. The solution resistance  $R_e$  is related to the water content, but the density of soil has no obvious effect on it.

In conclusion, the electrochemical parameters are closely related to the compaction parameters of loessial silt. When the electrochemical parameters of the effective stage on the compaction curve under a certain compaction energy are known, the compaction degree of compacted soil can be detected and evaluated using EIS, which is an efficient and nondestructive method.

#### 4. CONCLUSIONS

In this paper,  $E = 2013.7 \text{ kJ/m}^3$  compacted loessial silt samples under five different water content conditions were tested by EIS, and the following conclusions were obtained:

(1) Electrochemical measurement is closely related to the content of the sample pore fluid. When the water content is low ( $w < w_{opt} - 2\%$ ), even though the soil sample is dense, there is no connection between the sample surface and the electrode contact surface. As a result, the effective contact surface between the sample and the test electrode could not be formed, and the EIS was disordered.

(2) The solution resistance  $R_e$  decreases with increasing water content. The charge transfer resistance  $R_{ct}$  decreases with increasing water content. When the water content is close to the optimal water content,  $Q_{dl}$  is closest to the ideal capacitance.

(3) The change rule of soil particle resistance  $R_s$  and  $C_s$  with the water content is similar to that of the dry density with the water content. The  $R_s$  and  $C_s$  values reach their peak at the optimal water content. A higher dry density corresponds to a more continuous grain arrangement. The overall impedance characteristics of solid particles are more obvious.

(4) The charge transfer resistance  $R_{ct}$  decreases with increasing water content and eventually tends to be stable. The difficulty of charge transfer is closely related to the resistance among particles. With an increase in the water content, the resistance among particles decreases and eventually stabilizes.

#### ACKNOWLEDGEMENTS:

This work is supported by the National Natural Science Foundation of China (No. 51178287, 51578359 and No.51208333) and Postgraduate Innovation Foundation of Shanxi Province (No. 2018BY055).

#### References

1. K. S. Chen, A. M. Sha, *Rock Soil Mech.*, 31 (2010) 1023.
2. L. Y. Peng, J. K. Liu and L. H. Chen, *Rock Soil Mech.*, 29 (2008) 2241.
3. A. Q. Shen, N. X. Zheng, Y. Su, X. W. Li, and X. H. Song, *China J. Highw. Transp.*, 13 (2000) 14.
4. X. M. Li, H. Zhang and Y. Z. Sun, *J. Xinyang Norm. Univ., Nat. Sci. Ed.*, 30 (2017) 478.
5. C. Liu, L. Ding, *Geol. Prospect.*, 38 (2002) 89.
6. H. J. Jing, B. Zhang, *Journal of Traffic and Transportation Engineering*, 4 (2004) 14.
7. K. G. Zhang, S. Y. Liu, Soil mechanics, China Architecture & Building Press, (2010) Beijing, China.
8. I. Martinez, C. Andrade, *Mater. Corros.*, 62 (2011) 932.
9. E. Barsoukov, J. R. Macdonald, Impedance Spectroscopy Theory, Experiment, and Application, John Wiley & Sons, (2005) Hoboken, New Jersey, America.
10. Y. J. Liu, Q. Jiang, C. Z. Zhao, T. T. Liu and X. P. Xu. *Concrete*, (2007) 8.
11. J. C. Hu, H. F. Wang, M. C. He and X. M. Sun, *Chin. J. Geotech. Eng.*, 29 (2007) 853.
12. S. Q. Peng, F. Wang and L. Fan, *Int. J. Electrochem. Sci.*, 14 (2019) 8611.
13. Y. Shen, J. T. Feng, W. Shi and C. C. Qiu, *Int. J. Electrochem. Sci.*, 14 (2019) 2136.
14. Y. B. Yan, Experimental Study on silt of Physical and Mechanical and Electrochemical properties effected by different pH, Taiyuan University of Technology, (2018) Taiyuan, China.
15. P. Han, P. J. Han, Y. B. Yan and X. H. Bai, *Int. J. Electrochem. Sci.*, 13 (2018) 10548.
16. M. R. Wang, P. J. Han, *Science Technology and Engineering*, 18 (2018) 90.
17. C. N. Cao, J. Q. Zhang, An Introduction to Electrochemical Impedance Spectroscopy, Science Press (2002) Beijing, China.
18. C. N. Cao, Principles of Electrochemistry of corrosion, Beijing Industrial Press (2008) Beijing, China.
19. Standard for Soil Test Method, China planning press (2019) Beijing.
20. Code for Design of Building Foundation, China building industry press (2011) Beijing.
21. R. E. Olson, *J. Geotech. Geoenviron. Eng.*, 124 (1998) 659.
22. Y. C. Liang, N. Hilal, P. Langston and V. Starov, *Adv. Colloid Interface Sci.*, 134-135 (2007) 151.
23. Z. H. Yu, Y. Y. Zheng, J. B. Zhang, C. Z. Zhang, D. H. Ma, L. Chen and T. Y. Cai, *Geoderma*, 362 (2020) 1.
24. H. Wu, X. G. Zhang, N. P. Yi and Z. H. Dai, *Chin. J. Rock Mech. Eng.*, 19 (2000) 199.

25. N. P. Yi, H. Wu, X. G. Zhang, Z. H. Dai and J. Cao, *J. Guangxi Univ., Nat. Sci. Ed.*, 25 (2000) 16.
26. X. L. Zhang, Y. F. Zhang and P. J. Han, *Science Technology and Engineering*, 16 (2016) 46.
27. R. Z. Xie, Study on Electrochemical Characteristics and Corrosive Mechanism of Sandy Soil Containing Soluble Sodium Salt, Taiyuan University of Technology, (2019) Taiyuan, China.
28. R. Akkouche, C. Rémazeilles, M. Barbalat, R. Sabot, M. Jeannin, and P. Refait, *J. Electrochem. Soc.*, 164 (2017) C626.
29. B. He, The Influence of Particle Size on The Electrochemical Corrosion Behavior of The Contaminated System and X70 Steel in NaCl Contaminated Sandy Environment, Taiyuan University of Technology, (2016) Taiyuan, China.
30. L. Q. Ren, Soil Adhesion Mechanics, China Machine Press, (2011) Beijing, China.
31. J. Q. Zhang, Electrochemical Measurement Technology, Chemical Industry Press, (2010) Beijing, China.
32. L. Q. Ren, C. Z. Liu, J. Tong and J. Q. Li, *Trans. Chin. Soc. Agric. Mach.*, 28 (1997) 5.
33. L. Q. Ren, C. Z. Liu, J. Tong and J. Q. Li, *Trans. Chin. Soc. Agric. Mach.*, 28 (1997) 2.

© 2020 The Authors. Published by ESG ([www.electrochemsci.org](http://www.electrochemsci.org)). This article is an open access article distributed under the terms and conditions of the Creative Commons Attribution license (<http://creativecommons.org/licenses/by/4.0/>).